Chinese Chemical Letters 37 (2026) 111963

Contents lists available at ScienceDirect

Chinese Chemical Letters

journal homepage: www.elsevier.com/locate/cclet

Lewis acid catalyzed enantioselective dearomative (3+2) cycloaddition of aromatic *N*-heterocycles with bicyclobutanes

Feng Wu[a,1], Yuanjiu Xiao[a,1], Mengran Wei[b,1], Guoqiang Wang[b,*], Jian-Jun Feng[a,*]

[a] State Key Laboratory of Chemo and Biosensing, Advanced Catalytic Engineering Research Center of the Ministry of Education, College of Chemistry and Chemical Engineering, Hunan University, Changsha 410082, China
[b] State Key Laboratory of Coordination Chemistry, Key Laboratory of Mesoscopic Chemistry of Ministry of Education, School of Chemistry and Chemical Engineering, Nanjing University, Nanjing 210093, China

ARTICLE INFO

Article history:
Received 10 June 2025
Revised 2 October 2025
Accepted 13 October 2025
Available online 14 October 2025

Keywords:
Bicyclo[1.1.0]butanes
Dearomatization
Cycloadditions
Bioisosteres
Asymmetric catalysis
Lewis acid

ABSTRACT

Given the emerging demand to "escape from flatland" for modern medicinal chemistry, both the catalytic construction of complex three-dimensional molecular architectures from planar aromatics and the bioisosteric substitution of aromatic ring with bicyclo[2.1.1]hexanes (BCHs) become increasingly valuable. Despite notable advancements in the cycloaddition reactions involving bicyclo[1.1.0]butanes (BCBs) and 2π-components, the application of easily accessible aromatic compounds in these transformations, particularly in an asymmetric manner, is still relatively unexplored. Herein, we report a nickel-catalyzed enantioselective polar dearomative (3 + 2) cycloaddition of BCBs with benzazoles and indoles. This protocol offers an efficient route for the synthesis of *N*,*S*- or *N*,*N*-heterocycles decorated fused aza-BCHs bearing two quaternary carbon centers. This approach stands out for its practicality and appeal due to the utilization of easily accessible starting materials and catalysts, broad substrate scope, easy scalability, and the employment of mild reaction conditions. Density functional theory (DFT) calculations offer crucial insights into the reaction mechanism and elucidate the factors governing the enantioselectivity within the dearomative cycloaddition process.

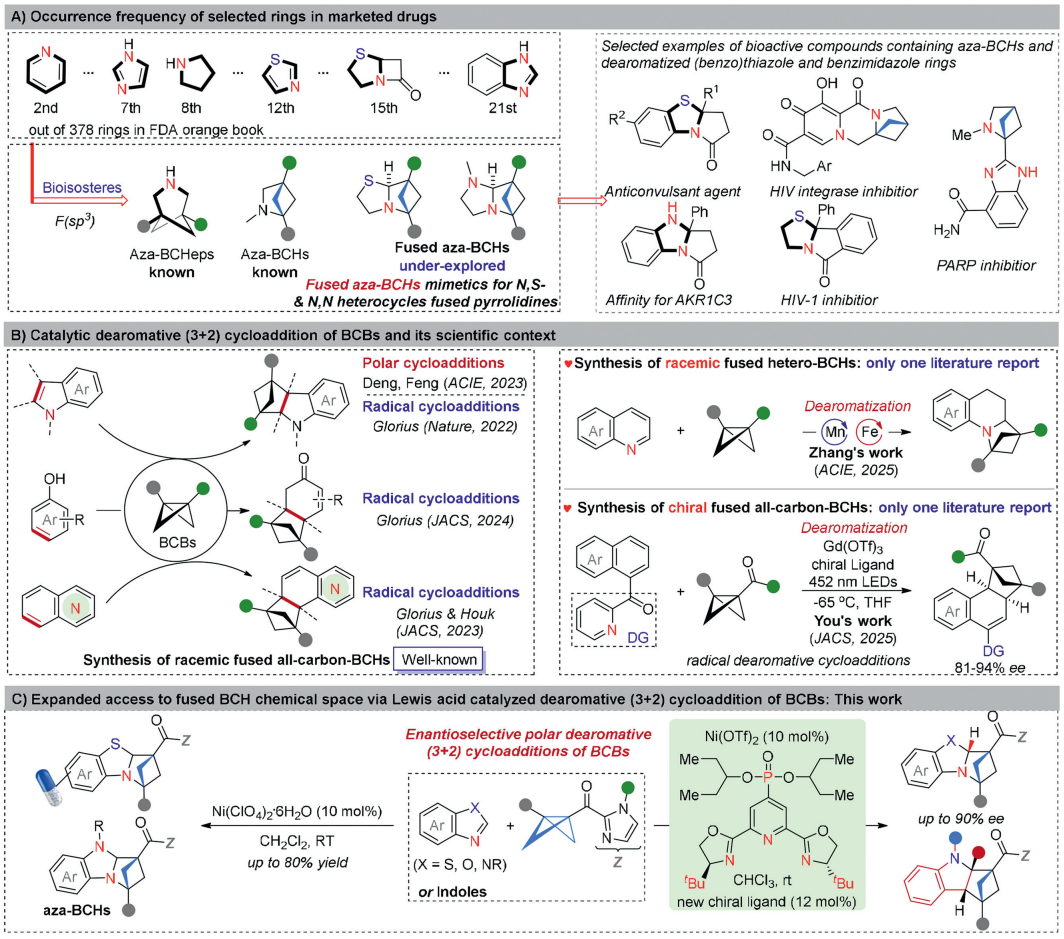
© 2025 Published by Elsevier B.V. on behalf of Chinese Chemical Society and Institute of Materia Medica, Chinese Academy of Medical Sciences.

Building on the success of the "escape from flatland" strategy in drug discovery, modifying the core scaffold of lead compounds to increase their saturation (Fsp^3) and complexity has emerged as a promising approach for enhancing clinical outcomes [1]. In this regard, research on the cycloaddition reactions of bicyclo[1.1.0]butanes (BCBs) has gained renewed interest [2–6], as these reactions enable the atom-economic synthesis of three-dimensional (3D) saturated bicyclo[n.1.1]alkanes—structures that act as effective or potential bioisosteres for flat arenes [7–9]. For instance, substituted bicyclo[2.1.1]hexanes (BCHs) with defined exit vectors are being recognized as C(sp^3)-rich bioisosteres for *ortho*- and *meta*-substituted benzenes [10,11]. Additionally, Mykhailiuk's groundbreaking research has demonstrated that their *N*- and *O*-incorporated analogs often impart enhanced pharmacokinetic and physicochemical properties [12–14]. Consequently, there is a growing interest among chemists in pursuit readily accessible coupling partners, such as alkenes [15–24], cyclic allenes [25], alkyne [20,26–27], ketenes [28], imines [29–33], aldehydes [34,35], α–ketoesters [36], thioketones [37,38], triazolinedione [39,40] and other related species [41], to facilitate the (3 + 2) cycloadditions of BCBs. In contrast, the reactions of BCBs with aromatic rings have lagged behind due to their kinetic inertness and thermodynamic stability [42–44].

Heteroaromatic rings and saturated *N*-heterocycles are ubiquitous structural motifs found in an array of natural products and small-molecule drugs, with pyridines the 2nd, imidazoles the 7th, pyrrolidines the 8th and thiazoles the 12th most prevalent in marketed drugs (Scheme 1A) [45]. Dearomatization reactions of arenes represent a unique approach for converting planar aromatic rings into diverse and valuable 3D scaffolds, thereby enhancing their saturation and structural complexity [46–50]. Among them, the integration of BCBs with dearomatization processes provides a streamlined and efficient means for constructing (hetero)cycle-fused BCH architectures. In 2022, Glorius reported the first dearomative [2π+2σ] cycloadditions of BCBs with indoles *via* a photoinduced energy transfer process [17]. Subsequently, radical [2π+2σ] cycloadditions of BCBs with a range of aromatic compounds, such as phenols [51], (iso)quinolones [52], quinazolines [52], and quinoxalines [52], have been extensively explored to expand the

* Corresponding authors.
E-mail addresses: wangguoqiang710@nju.edu.cn (G. Wang), jianjunfeng@hnu.edu.cn (J.-J. Feng).
[1] These authors contributed equally to this work.

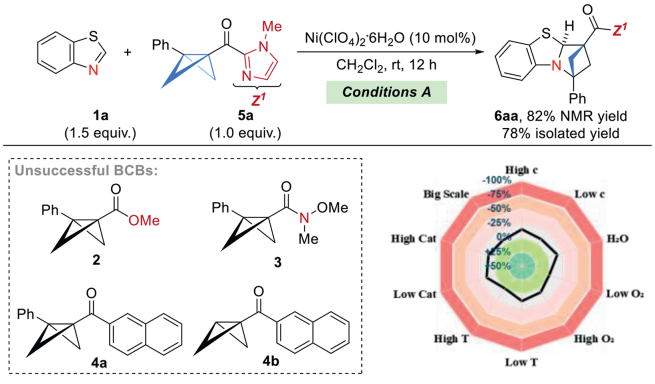
https://doi.org/10.1016/j.cclet.2025.111963
1001-8417/© 2025 Published by Elsevier B.V. on behalf of Chinese Chemical Society and Institute of Materia Medica, Chinese Academy of Medical Sciences.



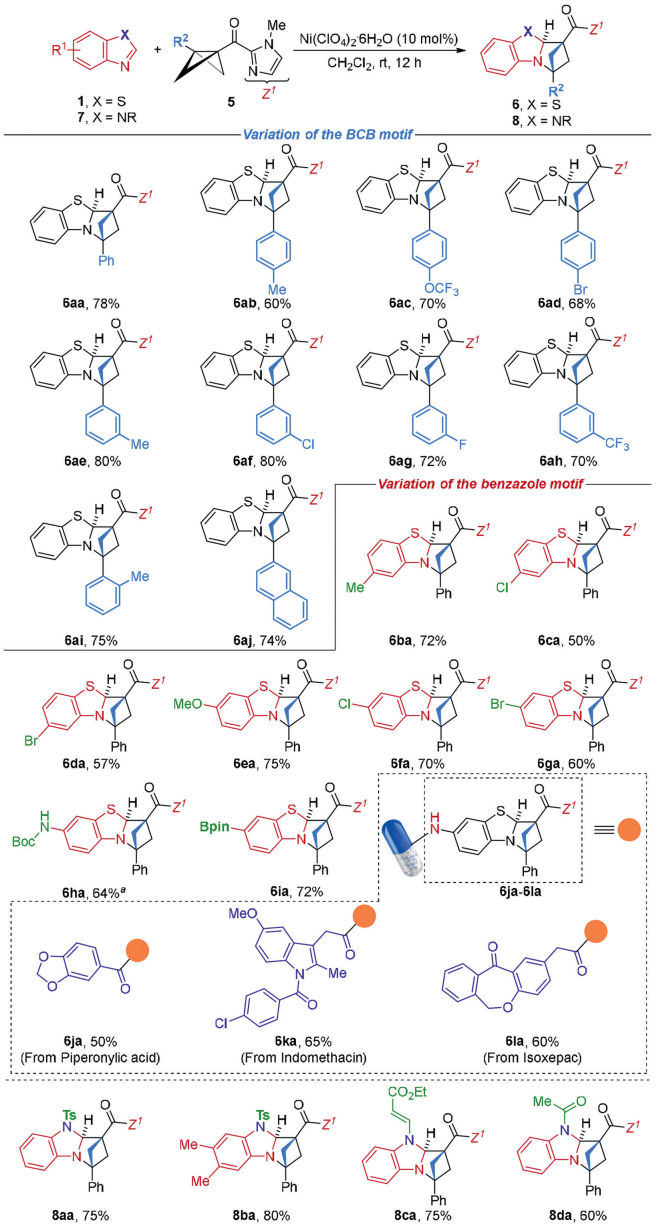
Scheme 1. Outline of this work.

chemical diversity of ring-fused all-carbon racemic BCHs (Scheme 1B, left). Despite significant progress in the field of dearomative (3+2) cycloadditions of BCBs, several challenges persist: (1) The scope of the 2π-component in polar dearomative (3+2) cycloaddition reactions of BCBs has been largely restricted to indoles [53,54]. (2) To date, only one study has been published on the synthesis of ring-fused hetero-BCHs through the dearomatization process. This remarkable achievement was realized by the Zhang group through a tandem hydrodearomatization/(3+2) cycloaddition reaction of aza-arenes with BCBs [55]. (3) Recently, there have been breakthroughs in radical and polar asymmetric (3+X) cycloadditions of BCBs [6,9,37,56–68]. However, the aromatic "X" component in these asymmetric reactions is both exceptionally rare and predominantly limited to activated aromatic rings [69–70]. While the You group reported the first enantioselective dearomative (3+2) photocycloaddition of BCBs in 2025 [71], the polar asymmetric dearomative (3+2) cycloaddition of BCBs has remained elusive (Scheme 1B, right). Here, we demonstrate the feasibility of an enantioselective polar dearomative (3+2) cycloaddition reaction of BCBs enabled by chiral Lewis acid catalysis. This is exemplified by the current enantioselective formal (3+2) cycloaddition of BCBs with aromatic *N*-heterocycles (Scheme 1C) [72–75].

Although Deng *et al.* reported Lewis acid-catalyzed (3+2) cycloaddition reactions of BCBs with electron-rich indoles for the synthesis of racemic BCHs in 2023 [53], the corresponding reactions involving benzazoles have not been reported yet, likely due to the lower nucleophilicity of benzazoles. Therefore, our primary goal is to achieve the cycloadditions of BCBs with benzothiazole **1a** to construct the racemic fused aza-BCH frameworks. Initially, we investigated the cycloadditions of **1a** with commonly used BCB ester **2** or BCB amide **3** in the presence of various Lewis and Brønsted acid catalysts. However, no desired cycloadduct was obtained and isomerization of BCB to the cyclobutene derivatives was observed. Gratifyingly, the treatment of BCB **4** containing a ketone moiety, which is a stronger electron-withdrawing substituent than esters and amides, could afford the aimed product in about 8% NMR yield with $Ni(ClO_4)_2$ as the catalyst. Based on these results, BCB **5a**, which contains a 2-acyl imidazole group, was chosen as the model substrate. After systematically screening Lewis acid catalysts, solvents and reaction temperatures, we were delighted to discover that the dearomative reaction produced **6aa** with 82% NMR yield under the optimized conditions A (Scheme 2 and Table S1 in Supporting information for details). Furthermore, the condition-based



Scheme 2. Reaction conditions for dearomative (3+2) cloadditions of BCBs.

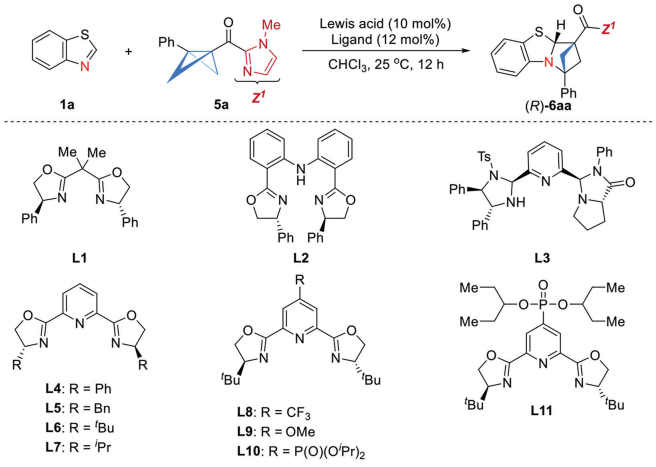


Scheme 3. Survey the scope of BCBs and benzazole derivatives. Unless otherwise noted, the reactions were performed with **1** or **7** (0.3 mmol), **5** (0.2 mmol) and $Ni(ClO_4)_2{\cdot}6H_2O$ (10 mol%) in CH_2Cl_2 (2 mL) at 25 °C for 12 h. The yields were isolated yields. [a] NMR yield of **6ha** The desired product was obtained together with benzothiazole **1h** which cannot be separated by chromatography.

sensitivity analysis [76] demonstrated that variations in moisture, catalyst loading, concentration, O_2 level, temperature, and scale do not significantly affect the reaction.

With optimized reaction conditions established, we initiated our exploration of the substrate scope of the dearomative (3 + 2) cycloaddition reaction (Scheme 3). The reaction of aromatic BCBs with different substituents on the phenyl moiety, including alkyl (methyl as in **6ab**, **6ae** and **6ai**), OCF_3 (**6ac**) and halogen (4-Br as in **6ad**; 3-Cl as in **6af**; 3-F as in **6ag**) groups, at either the *para*, *meta*, or *ortho* position, also proceeded with good efficiency (**6ab**–**6ai**). Despite of the electronic property of the substituents, all the reactions with **1a** proceeded smoothly (60 %–80 % yield). Notably, BCB bearing a strong electron-withdrawing trifluoromethyl group afforded cycloadduct **6ah** in good yield. This result suggests that, unlike the previous Lewis acid-catalyzed (3 + 2) cycloadditions of BCBs, a benzylic carbocation intermediate might not be

Table 1
Optimization of reaction conditions.[a]



Entry	Lewis acid	Ligand	Yield (%)[b]	er[c]
1	$Ni(OTf)_2$	**L1**	81	65:35
2	$Ni(OTf)_2$	**L2**	29	50:50
3	$Ni(OTf)_2$	**L3**	80	53:47
4	$Ni(OTf)_2$	**L4**	21	56.5:43.5
5	$Ni(OTf)_2$	**L5**	28	74:26
6	$Ni(OTf)_2$	**L6**	75	92.5:7.5
7	$Ni(OTf)_2$	**L7**	13	84:16
8	$Zn(OTf)_2$	**L6**	65	81.5:18.5
9	$Cu(OTf)_2$	**L6**	23	73.5:26.5
10	$Co(OTf)_2$	**L6**	50	84.5:15.5
11[d]	$Ni(OTf)_2$	**L6**	55	89.5:10.5
12[e]	$Ni(OTf)_2$	**L6**	51	90:10
13	$Ni(OTf)_2$	**L8**	83	92:8
14	$Ni(OTf)_2$	**L9**	58	85.5:14.5
15	$Ni(OTf)_2$	**L10**	88	93.5:6.5
16	$Ni(OTf)_2$	**L11**	90	93.5:6.5

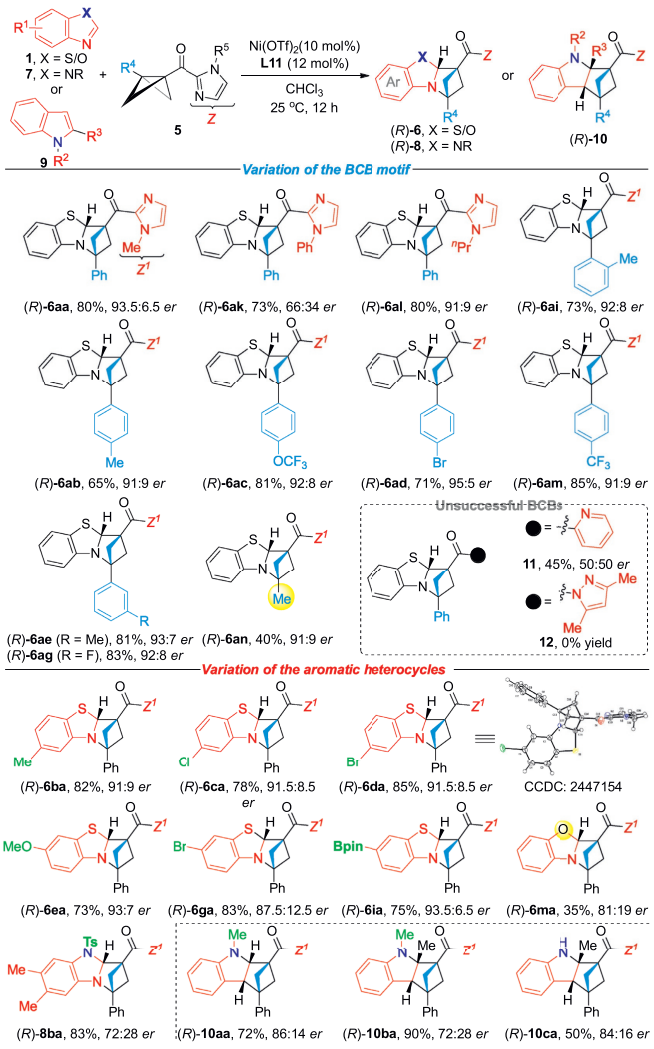
[a] Reaction conditions B: **1a** (0.15 mmol), **5a** (0.10 mmol), Lewis acid (10 mol%), ligand (12 mol%), $CHCl_3$ (2 mL), 25 °C under N_2 for 12 h.
[b] NMR yield with CH_2Br_2 as an internal standard.
[c] Based on chiral HPLC analysis.
[d] Performed in THF.
[e] Run at 0 °C.

generated in our work. Moreover, naphthyl substituted BCB (**5j**) was compatible, giving the corresponding dearomatized benzothiazole **6aj** in reasonable yield. Subsequently, various benzothiazoles were tested under the optimized reaction conditions. Benzothiazole derivatives (**6ba**–**6la**) with a variety of functional groups on the phenyl ring, including halogen (**6ca**, **6da**, **6fa** and **6ga**), a methoxy group (**6ea**), and an amide (**6ha**), were also compatible with our catalytic system. Notably, benzothiazole **1i** bearing a boronic acid pinacol ester (Bpin) group was converted to the desired product **6ia** in 72 % yield, offering many opportunities for further diversification. Importantly, our protocol allowed the incorporation of the *N*,*S*-heterocycles, which are among the most common structural motifs in FDA-approved small-molecule drugs, into bioactive molecules such as piperonylic acid, indomethacin and isoxepac (**6ja**–**6la**). Aside from benzothiazoles, a series of N^1-substituted benzimidazole derivatives could undergo dearomative cycloaddition smoothly to afford the corresponding products **8aa**-**8da** in moderate to good yield. Substrates with a N^1-tosyl group showed higher yield than the other substrates bearing a N^1-acyl group (**8aa** and **8ba** *versus* **8da**). Furthermore, the Tosyl group in **7a** could be replaced by a vinyl substituent (**8ca**) still maintaining a decent yield.

Following the establishment of non-asymmetric dearomative (3 + 2) cycloadditions of benzazoles with BCBs, we then advanced to develop the asymmetric dearomative version. As shown in Table 1 (for details, see Table S2 in Supporting information), the

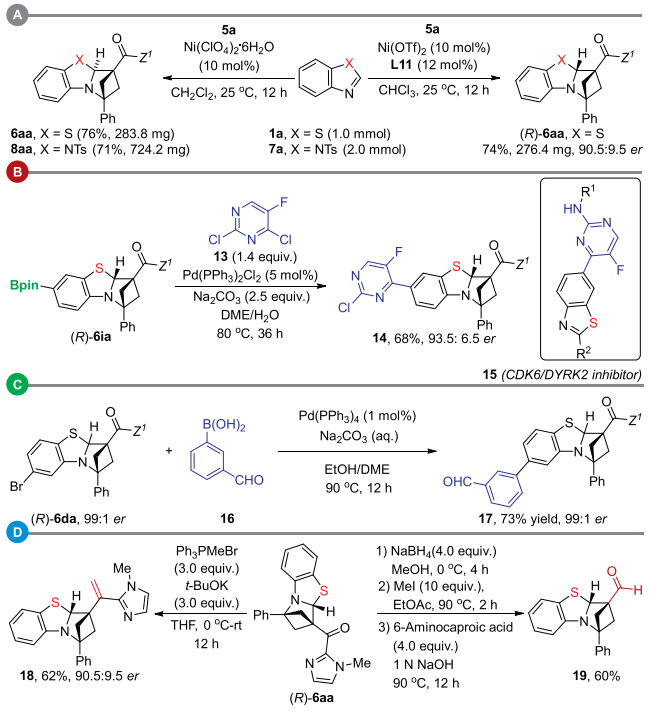
treatment of **1a** and **5a** in the presence of $Ni(OTf)_2$ and **L1,** yielded **6aa** with an enantiomeric ratio (*er*) of 65:35 (Table 1, entry 1). This observation prompted us to explore various chiral ligands for the cycloaddition reaction (entries 2–7 and 13–16). Unfortunately, replacement of the BOX ligand **L1** with the bis(oxazolinylphenyl)amide ligand **L2** and the PyIPI ligand **L3** [77], which had proven effective in previous asymmetric (3 + 2) and (3 + 3) cycloadditions of BCBs [59,67], resulted in low enantioselectivity (entries 2 and 3). Subsequently, we redirected our efforts to alternative PyBox ligands (**L4-L7**). Among these, the combination of $Ni(OTf)_2$ with ligand **L6** was found to be the most effective, yielding the desired product **6aa** in 75 % yield with 92.5:7.5 *er* (entry 6 *versus* 4–5, 7). Next, a systematic evaluation of commonly employed metal-Lewis acids, solvents, and reaction temperatures was conducted; however, these modifications failed to improve the *er* values (entries 8–12). Inspired by Zhou's work demonstrating that C4 modification of PyBox ligands with electronically and sterically diverse groups enhances enantioselectivity in transition metal catalyzed azide-alkyne cycloadditions [78], we evaluated a series of C4-substituted PyBox derivatives (**L8-L11**, entries 13–16). Notably, the combination of $Ni(OTf)_2$ and **L11** proved highly effective, afforded product **6aa** in 90 % yield with 93.5:6.5 *er* values (entry 16).

Under optimal reaction condition, we initiated our investigations by screening the 2-acyl imidazole group at BCB (Scheme 4).



Scheme 4. Scope of Lewis acid catalyzed enantioselective dearomative (3 + 2) cloadditions of BCBs. Conditions B: **1**, **7** or **9** (0.3 mmol), **5** (0.2 mmol), $Ni(OTf)_2$ (10 mol%) and **L11** (12 mol%) in $CHCl_3$ (2 mL) at 25 °C for 12 h; Isolated yield.

The methyl *N*-substituted imidazole **5a** was marginally better in overall yields and enantioselectivity, as compared with phenyl *N*-substituted imidazole **5k** and *n*-propyl *N*-substituted imidazole **5l** (**6aa** *versus* **6ak**, **6al**). So we then focused on the evaluation of a variety of 1,3-disubstituted BCBs bearing *N*-methylimidazole groups. BCBs bearing trifluoromethoxy (**5c**) and trifluoromethyl (**5m**) groups on the aryl ring, which are commonly employed in pharmaceutical and agrochemical contexts, effectively participated in the reaction, yielding the desired products with good yields and enantioselectivity (**6ac** and **6am**). In contrast, substrate **5b**, which contains an electron-donating group, resulted in lower yields and *er* compared to those bearing electron-withdrawing groups (**6ab** *versus* **6ac-6ad**, **6am**). Additionally, the incorporation of halogen atoms at the *para*- or *meta*-positions of the benzene ring did not adversely affect the reaction efficiency, as demonstrated by the successful synthesis of **6ad** and **6ag**. Furthermore, the use of substrate **5i**, featuring a methyl substituent at the *ortho*-position, also afforded good product yield and 92:8 *er* (**6ai**). BCB **1n**, which bears a methyl group at the β-position of the BCB scaffold, is also a suitable substrate for furnishing the desired product **6an** in 40 % yield and 91:9 *er*. Although acyl pyrazole-decorated BCB did not generate the corresponding product **12**, the (3 + 2) cycloaddition of acyl pyridine-decorated BCB with **1a** afforded **11** in 45 % yield but with 0 % *ee*. These results indicate that forming a stable chiral environment *via* chelation of a bidentate acyl imidazole group to chiral Lewis acid catalyst is essential for enantioselective control. For benzothiazole derivatives, regardless of whether they are substituted with a methyl group (**6ba**), halogens (**6ca**, **6da**, **6ga**), a methoxy group (**6ea**), or a boronic acid pinacol ester (Bpin) (**6ia**), were well tolerated and afforded the desired products with good efficiency (73 %–85 % yield) and enantioselectivity (87.5:12.5 to 93.5:6.5 *er*). Through a single recrystallization, the optical purity of compound **6da** was enhanced to over 99:1 *er*. Moreover, the structure and absolute configuration of (*R*)-**6da** were definitively established *via* X-ray crystallographic analysis. Notably, N^1-tosyl-substituted benzimidazole was likewise transformed into the desired product **8ba** in 83 % yield, albeit with a lower *er*. Notably,

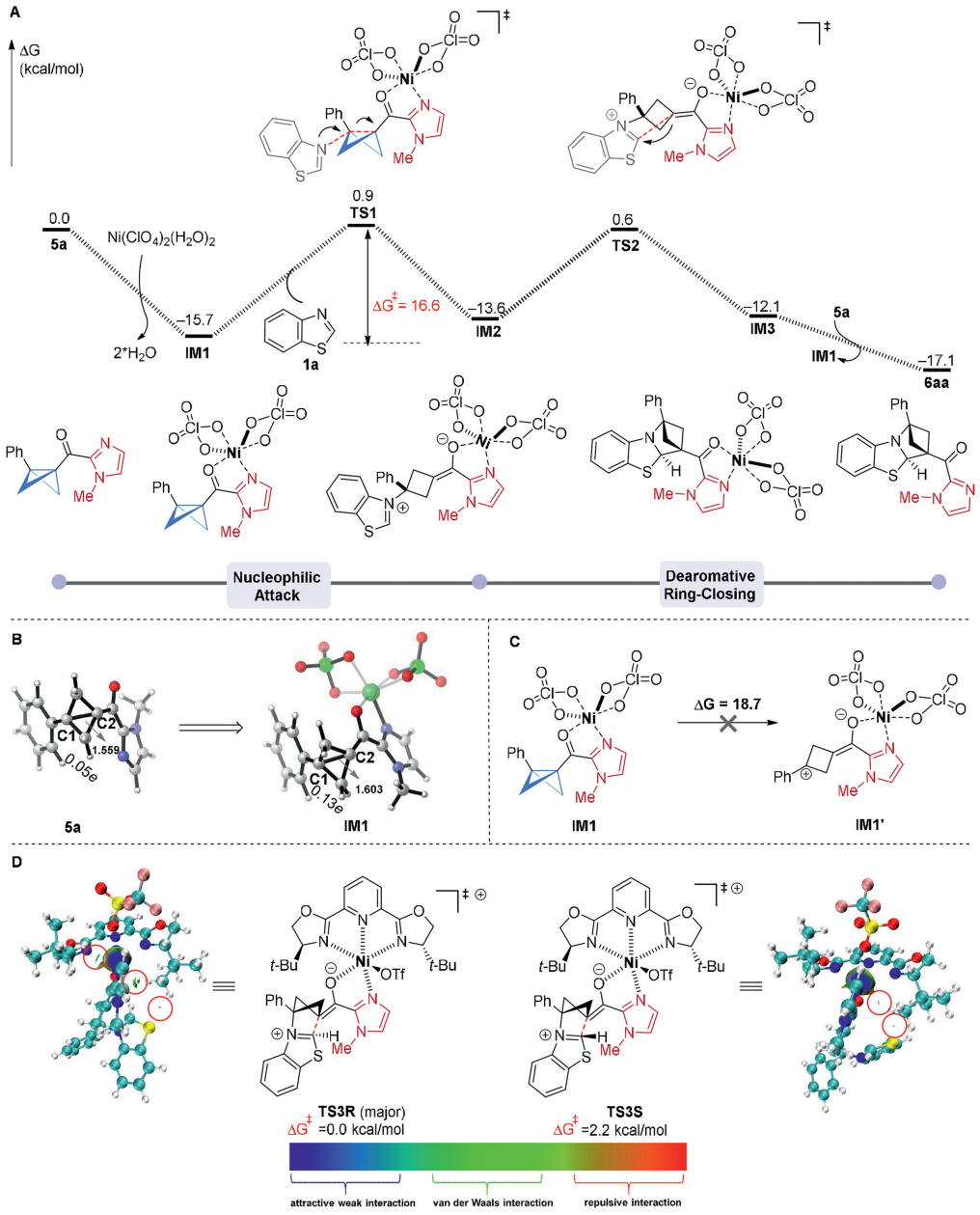


Scheme 5. Scaled-up preparation and synthetic transformations.

this reaction was successfully extended to benzoxazole (**6ma**) and indoles (**10aa**-**10ca**), yielding the corresponding cycloadducts in moderate to excellent yields, with enantiomeric ratios ranging from 72:28 to 86:14.

The scaled-up synthesis of the dearomatized benzothiazole **6aa** and benzimidazole **8aa** proceeded readily and delivered a comparable yield and enantioselectivity, showing the practicality of the protocol (Scheme 5A). Benzothiazoles **15** containing pyrimidine groups are a selective CDK6/DYRK2 inhibitor and showed good antitumor activity [79]. **6ia** can undergo Suzuki cross-coupling reaction with pyrimidine **13** smoothly to give corresponding dearomatized benzothiazole **14** as the analogues of CDK6/DYRK2 inhibitor **15** (Scheme 5B). Furthermore, Suzuki coupling of (*R*)-**6da** with arylboronic acid **16** is also facile, leading to the formation of functionalized **17** (Scheme 5C). In addition, cycloadduct **6aa** could be converted into dearomatized benzimidazole derivatives **18** by Wittig olefination reaction. Subsequent cleavage of the imidazole moiety gave rise to the desired aldehyde **19** in 60 % yield (Scheme 5D).

To further elucidate the mechanistic details of this reaction, DFT calculations on a model reaction of benzothiazole **1a** with BCB **5a** using $Ni(ClO_4)_2$ as the catalyst were conducted with B3LYP-D3 functional using the PCM model to treat the solvent effect (basis set details are collected in Supporting information) [80–84]. 3D structures were generated with CYLview software [85]. The unrestricted method was applied for the nickel complex. The reaction starts with the complexation of BCB **5a** with $Ni(ClO_4)_2$. Both the singlet and triplet geometries of **5a**-$Ni(ClO_4)_2$ complex were optimized. High-spin species **IM1** adopts an octahedral nickel center with the 2-acyl imidazole group of **5a** in a bidentated coordina-



Scheme 6. DFT calculation on the reaction mechanism. (A): Reaction coordinate for the $Ni(ClO_4)_2$-catalyzed dearomative (3 + 2) cycloaddition of benzothiazole **1a** with bicyclobutanes **5a** (Gibbs free energies are in kcal/mol); (B): Optimized structures of bicyclobutane **5a** and $Ni(ClO_4)_2$–**5a** complex **IM1** (Distances are shown in Å; Natural charges in C1 position are in a.u.). Color code: H, white; C, gray; N, blue; O, red; N, blue; Cl, green; Ni, dark green. (C): Thermodynamic difference between **IM1** and zwitterionic enolate intermediate **IM1'**. (D): DFT calculation and IGMH analysis on the key stereoselectivity-determining step with (*S*)-**L6** as the ligand.

tion fashion. The low-spin complex tends to be a square-planar structure. Our computations revealed that **5a**-$Ni(ClO_4)_2$ complex is preferred in the high spin ground state; and it is calculated to be 27.7 kcal/mol more favorable than the singlet state (Fig. S1 in Supporting information). According to our DFT calculations, this dearomative (3 + 2) cycloaddition reaction proceeds through a nucleophilic-type process.

As shown in Scheme 6A, the formation of **IM1** is exergonic by 15.7 kcal/mol. In **IM1**, the C1-C2 bond in BCB ring is elongated from 1.559 Å in **5a** to 1.603 Å (Scheme 6B). NPA charge calculations reveal that the benzylic carbon in **IM1** (0.13 e) is more positively charged than that in **5a** (0.05 e). These results indicate that the nucleophilicity of the benzylic carbon atom in BCB ring is enhanced upon the complexation of **5a** with $Ni(ClO_4)_2$. Then, the nucleophilic attack of benzothiazole **1a** at the C1 atom of **IM1** (*via* transition state **TS1**) leads to the formation of zwitterionic enolate intermediate **IM2**. In **TS1**, the formation of C1-N occurs concertedly with the cleavage of C1-C2 bond in BCB ring. Such a process is slightly endergonic by 2.1 kcal/mol with an activation barrier of 16.6 kcal/mol (with respect to **IM1** as the energy reference). Subsequently, **IM2** undergoes an intramolecular nucleophilic cyclization *via* **TS2** to give the cycloaddition complex **IM3** ($\Delta G^{\ddagger} = 16.3$ kcal/mol). Finally, ligand exchange between **5a** and **IM3** gives the dearomative heterocycle **6aa**. Along the whole free energy profile, the nucleophilic ring-opening step is the rate-limiting step with a barrier of 16.6 kcal/mol, which is consistent with our experimental observation that the reaction took place smoothly at room temperature.

In addition to the proposed Ni-catalyzed nucleophilic attack mechanism (*via* **TS1**), a stepwise mechanism proceeding through the direct cleavage of C1-C2 bond in **IM1** with the assistance of $Ni(ClO_4)_2$, generating zwitterionic enolate intermediate **IM1'**, was also considered (Scheme 6C). However, the formation of **IM1'** is endothermic by 18.7 kcal/mol, which is even higher than **TS1**. Therefore, the pathway involving the nucleophilic reaction between benzothiazole **1a** and zwitterionic enolate intermediate **IM1'** can be excluded. The employment of a BCB bearing a strong electron-withdrawing trifluoromethyl group at the phenyl ring also delivered the corresponding product in good yield (**6ah** and **6am**), which supports the involvement of a concerted ring-opening process during the reaction.

Furthermore, DFT calculations were performed to elucidate the origin of stereoselectivity for the asymmetric (3 + 2) cycloaddition of benzothiazole with bicyclobutane using (*S*)-**L6** as the ligand (Figs. S3 and S4 in Supporting information for details). Specifically, the key stereoselectivity-determining step, C–C bond formation was theoretically investigated. As shown in Scheme 6D, the Gibbs free energy of the transition state leading to (*R*)-**6aa** (**TS3R**) is predicted to be 2.2 kcal/mol lower than the transition state (**TS3S**) related to (*S*)-enantiomer. This barrier difference is qualitatively consistent with the experimentally observed enantioselectivity. To elucidate the origin of this energy difference between the two transition states, we further employed the independent gradient model based on the Hirshfeld partition (IGMH) to analyze the potential weak interactions [86–89]. It was found that in comparison with **TS3S**, energetically favored **TS3R** has multiple and stronger intensity of C–H···π interactions between the (*S*)-**L6** ligand and substrate (highlighted with red circles), indicating that enantioselectivity is primarily governed by non-covalent interactions.

In summary, by using a nickel-Lewis acid catalyst, we have succeeded in developing the polar dearomative (3 + 2) cycloaddition of BCBs with diverse aromatic *N*-heterocycles, enabling the synthesis of ring-fused (hetero-)BCHs. The reaction proceeds through an unusual concerted nucleophilic ring opening of BCBs with benzazoles and indoles, followed by the formation of a zwitterionic enolate intermediate (**IM2**) and subsequent intramolecular dearomative nucleophilic cyclization processes. This protocol features 100 % atom utilization, mild reaction conditions, high yields, broad compatibility with various functional groups, and ease of scalability. Moreover, the applicability of this method was demonstrated in the late-stage modification of drug-like molecules. Notably, we developed the enantioselective catalysis of this reaction by employing a nickel-based chiral Lewis acid catalytic system, achieving a maximum of 95:5 *er*. This study reports a rare instance of Lewis acid-catalyzed asymmetric dearomative (3 + 2) cycloaddition involving BCBs, setting the stage for the enantioselective construction of chiral ring-fused aza-BCHs via chiral Lewis acid catalysis.

Declaration of competing interest

The authors declare that they have no known competing financial interests or personal relationships that could have appeared to influence the work reported in this paper.

CRediT authorship contribution statement

Feng Wu: Writing – original draft, Investigation, Data curation. **Yuanjiu Xiao:** Writing – original draft, Investigation, Data curation. **Mengran Wei:** Software, Investigation, Data curation. **Guoqiang Wang:** Writing – review & editing, Writing – original draft, Software, Methodology, Investigation. **Jian-Jun Feng:** Writing – review & editing, Writing – original draft, Resources, Methodology, Funding acquisition, Data curation, Conceptualization.

Acknowledgments

We are grateful to the National Natural Science Foundation of China (No. 22471068 to J.-J. Feng, No. 22273035 to G.Q. Wang) and Fundamental Research Funds for the Central Universities for financial support. All theoretical calculations were performed at the High-Performance Computing Center (HPCC) of Nanjing University. The ^{1}H, ^{13}C NMR spectra, X-ray and HRMS (ESI) were performed at Analytical Instrumentation Center of Hunan University. G.Q. Wang acknowledges the financial support by Engineering Research Center of Photoresist Materials, Ministry of Education.

Supplementary materials

Supplementary material associated with this article can be found, in the online version, at doi:10.1016/j.cclet.2025.111963.

References

[1] F. Lovering, J. Bikker, C. Humblet, J. Med. Chem. 52 (2009) 6752–6756.
[2] M. Golfmann, J.C.L. Walker, Commun. Chem. 6 (2023) 9.
[3] M.A.A. Walczak, T. Krainz, P. Wipf, Acc. Chem. Res. 48 (2015) 1149–1158.
[4] S.J. Sujansky, X.S. Ma, Asian J. Org. Chem. 13 (2024) e202400045.
[5] X. Zhou, Y. Hu, Y. Huang, et al., Chem. Commun. 61 (2025) 23–32.
[6] Y.J. Xiao, L. Tang, X.C. Yang, et al., CCS Chem. 7 (2025) 1903–1934.
[7] P.K. Mykhailiuk, Org. Biomol. Chem. 17 (2019) 2839–2849.
[8] J. Tsien, C. Hu, R.R. Merchant, et al., Nat. Rev. Chem. 8 (2024) 605–627.
[9] X.C. Yang, J.J. Wang, Y.J. Xiao, et al., Angew. Chem. Int. Ed. (2025) e202505803.
[10] V.V. Levterov, Y. Panasyuk, V.O. Pivnytska, et al., Angew. Chem. Int. Ed. 59 (2020) 7161–7167.
[11] P. Garrido-García, I. Quirós, P. Milán-Rois, et al., Nat. Chem. 17 (2025) 734–745.
[12] A. Denisenko, P. Garbuz, N.M. Voloshchuk, et al., Nat. Chem. 15 (2023) 1155–1163.
[13] D. Dibchak, M. Snisarenko, A. Mishuk, et al., Angew. Chem. Int. Ed. 62 (2023) e202304246.
[14] V.V. Levterov, Y. Panasiuk, O. Shablykin, et al., Angew. Chem. Int. Ed. 63 (2024) e202319831.
[15] A. Cairncross, E.P. Blanchard Jr., J. Am. Chem. Soc. 88 (1966) 496–504.
[16] P. Wipf, M.A.A. Walczak, Angew. Chem. Int. Ed. 45 (2006) 4172–4175.
[17] R. Kleinmans, T. Pinkert, S. Dutta, et al., Nature 605 (2022) 477–482.
[18] R.Y. Guo, Y.C. Chang, L. Herter, et al., J. Am. Chem. Soc. 144 (2022) 7988–7994.
[19] S. Agasti, F. Beltran, E. Pye, et al., Nat. Chem. 15 (2023) 535–541.
[20] M. Xu, Z.J. Wang, Z.H. Sun, et al., Angew. Chem. Int. Ed. 61 (2022) e202214507.
[21] Y. Liu, S. Lin, Y. Li, et al., ACS Catal. 13 (2023) 5096–5103.

[22] J.J. Wang, L. Tang, Y.J. Xiao, et al., Angew. Chem. Int. Ed. 63 (2024) e202405222.
[23] Y.H. Liu, Z.X. Wu, J.R. Shan, et al., Nat. Commun. 15 (2024) 4374.
[24] Z.R. Lin, H.S. Ren, X.B. Lin, et al., J. Am. Chem. Soc. 146 (2024) 18565–18575.
[25] A.T. Meza, C.A. Rivera, H.L. Shao, et al., Nature 640 (2025) 683–690.
[26] Q.Q. Hu, L.Y. Wang, X.H. Chen, et al., Angew. Chem. Int. Ed. 63 (2024) e202405781.
[27] D. Sarkar, S. Deswal, R.C. Das, et al., Chem. Sci. 15 (2024) 16243–16249.
[28] N. Radhoff, C.G. Daniliuc, A. Studer, Angew. Chem. Int. Ed. 62 (2023) e202304771.
[29] K. Dhake, K.J. Woelk, J. Becica, et al., Angew. Chem. Int. Ed. 61 (2022) e202204719.
[30] F. Wu, W.B. Wu, Y.J. Xiao, et al., Angew. Chem. Int. Ed. 63 (2024) e202406548.
[31] J.T. Che, W.Y. Ding, H.B. Zhang, et al., Nat. Chem. 17 (2025) 393–402.
[32] X.G. Zhang, J.J. Chen, Z.Y. Zhou, et al., Chem Catal. 5 (2025) 101295.
[33] M. Yan, Z. Ye, P. Lu, Chin. Chem. Lett. 36 (2025) 110540.
[34] Y.J. Liang, F. Paulus, C.G. Daniliuc, et al., Angew. Chem. Int. Ed. 62 (2023) e202305043.
[35] S.Y. Tang, Z.J. Wang, J.J. Wu, et al., Chem. Sci. 16 (2025) 11908–11917.
[36] Y.J. Liang, R. Kleinmans, C.G. Daniliuc, et al., J. Am. Chem. Soc. 144 (2022) 20207–20213.
[37] L. Tang, W.J. Bai, K.J. Wang, et al., ACS Catal. 15 (2025) 7877–7890.
[38] D.A. Knyazev, M. Georgea, D.B. Werz, Chem. Sci. 16 (2025) 8588–8593.
[39] M. Wang, Y.C. Huang, C.Y. Li, et al., Org. Chem. Front. 9 (2022) 2149–2153.
[40] B.D. Schwartz, A.P. Smyth, P.E. Nashar, et al., Org. Lett. 24 (2022) 1268–1273.
[41] K.J. Woelk, K. Dhake, N.D. Schley, et al., Chem. Commun. 59 (2023) 13847–13850.
[42] Z. Zhang, X. Cao, X. Song, et al., Chin. Chem. Lett. 34 (2023) 107779.
[43] Z.X. Zhang, X. Wang, J.T. Jiang, et al., Chin. Chem. Lett. 34 (2023) 107647.
[44] Y.H. Miao, Z.X. Zhang, X.Y. Huang, et al., Chin. Chem. Lett. 35 (2024) 108830.
[45] R.D. Taylor, M. MacCoss, A.D.G. Lawson, J. Med. Chem. 57 (2014) 5845–5859.
[46] C.X. Zhuo, W. Zhang, S.L. You, Angew. Chem. Int. Ed. 51 (2012) 12662–12686.
[47] Q.P. Ding, X.L. Zhou, R.H. Fan, Org. Biomol. Chem. 12 (2014) 4807–4815.
[48] W.C. Wertjes, E.H. Southgate, D. Sarlah, Chem. Soc. Rev. 47 (2018) 7996–8017.
[49] F.T. Sheng, J.Y. Wang, W. Tan, et al., Org. Chem. Front. 7 (2020) 3967–3998.
[50] C. Zheng, S.L. You, ACS Cent. Sci. 7 (2021) 432–444.
[51] S. Dutta, D. Lee, K. Ozols, et al., J. Am. Chem. Soc. 146 (2024) 2789–2797.
[52] R. Kleinmans, S. Dutta, K. Ozols, et al., J. Am. Chem. Soc. 145 (2023) 12324–12332.
[53] D.S. Ni, S. Hu, X.Y. Tan, et al., Angew. Chem. Int. Ed. 62 (2023) e202308606.
[54] L. Tang, Y.J. Xiao, F. Wu, et al., Angew. Chem. Int. Ed. 62 (2023) e202310066.
[55] J. Yang, B.X. Yao, H.F. Jiang, et al., Angew. Chem. Int. Ed. 64 (2025) e202505060.
[56] M. de Robichon, T. Kratz, F. Beyer, et al., J. Am. Chem. Soc. 145 (2023) 24466–24470.
[57] Q.Q. Fu, S.S. Cao, J.H. Wang, et al., J. Am. Chem. Soc. 146 (2024) 8372–8380.
[58] X.H. Wang, R.K. Gao, X.X. Li, J. Am. Chem. Soc. 146 (2024) 21069–21077.
[59] W.B. Wu, B. Xu, X.C. Yang, et al., Nat. Commun. 15 (2024) 8005.
[60] T.Z. Qin, M.Y. He, W.W. Zi, Nat. Synth. 4 (2025) 124–133.
[61] X.G. Zhang, Z.Y. Zhou, J.X. Li, et al., J. Am. Chem. Soc. 146 (2024) 27274–27281.
[62] J. Jeong, S. Cao, H.J. Kang, et al., J. Am. Chem. Soc. 146 (2024) 27830–27842.
[63] J. Zhang, J.Y. Su, H.L. Zheng, et al., ACS Catal. 14 (2024) 17837–17849.
[64] Y.J. Li, Z.L. Wu, Q.S. Gu, et al., J. Am. Chem. Soc. 146 (2024) 34427–34441.
[65] S. Dutta, C.G. Daniliuc, C. Muck-Lichtenfeld, et al., J. Am. Chem. Soc. 147 (2025) 4249–4257.
[66] H.S. Ren, Z.R. Lin, T.X. Li, et al., ACS Catal. 15 (2025) 4634–4643.
[67] H.X. He, F. Wu, X. Zhang, et al., Angew. Chem. Int. Ed. 64 (2025) e202416741.
[68] T.Z. Qin, W.W. Zi, Chin. Chem. Lett. 37 (2026) 111072.
[69] Y.J. Xiao, F. Wu, L. Tang, et al., Angew. Chem. Int. Ed. 63 (2024) e202408578.
[70] X.C. Yang, F. Wu, W.B. Wu, et al., Chem. Sci. 15 (2024) 19488–19495.
[71] W.J. Shen, X.X. Zhou, M.Z. Li, et al., J. Am. Chem. Soc 147 (2025) 11667–11674.
[72] D.C. Wang, M.S. Xie, H.M. Guo, et al., Angew. Chem. Int. Ed. 55 (2016) 14111–14115.
[73] Z.P. Yang, C. Zheng, L. Huang, et al., Angew. Chem. Int. Ed. 56 (2017) 1530–1534.
[74] M.C. Zhang, D.C. Wang, M.S. Xie, et al., Chem 5 (2019) 156–167.
[75] S.S. Zhang, R.X. Wang, Q. Gu, et al., CCS Chem. 7 (2025) 194–204.
[76] L. Pitzer, F. Schäfers, F. Glorius, Angew. Chem. Int. Ed. 58 (2019) 8572–8576.
[77] H.-X. Wang, C. Yang, B.Y. Xue, et al., Nat. Commun. 14 (2023) 2270.
[78] K. Liao, Y. Gong, R.Y. Zhu, et al., Angew. Chem. Int. Ed. 60 (2021) 8488–8493.
[79] P. Yang, H. Hao, Y. Xiao, et al., (Jiangsu Tasly Diyi Pharmaceutical Co., Ltd.), Patent, Wo 2022/156059 A1, 2022.
[80] C. Lee, W. Yang, R.G. Parr, Phys. Rev. B 37 (1988) 785.
[81] A.D. Becke, J. Chem. Phys. 98 (1993) 5648–5652.
[82] S. Grimme, J. Antony, S. Ehrlich, et al., J. Chem. Phys. 132 (2010) 154104.
[83] S. Grimme, S. Ehrlich, L. Goerigk, J. Comput. Chem. 32 (2011) 1456–1465.
[84] J. Tomasi, M. Persico, Chem. Rev. 94 (1994) 2027–2094.
[85] C.Y. Legault, CYLview, 1.0b; Université de Sherbrooke, 2009. downloaded on February 28, 2021 from http://www.cylview.org.
[86] W. Humphrey, A. Dalke, K. Schulten, J. Mol. Graph. 14 (1996) 33–38 http://www.ks.uiuc.edu/Research/vmd.
[87] C. Lefebvre, G. Rubez, H. Khartabil, et al., Phys. Chem. Chem. Phys. 19 (2017) 17928–17936.
[88] T. Lu, F. Chen, J. Comput. Chem. 33 (2012) 580–592.
[89] T. Lu, Q. Chen, J. Comput. Chem. 43 (2022) 539–555.